

Silicon-based spin and charge quantum computation

Belita K oiller,¹ Xuedong Hu,² R.B. Capaz,¹ A.S. Martins,³ and S. Das Sarma⁴

¹Instituto de Física, Universidade Federal do Rio de Janeiro,
Cx. Postal 68.528, Rio de Janeiro, 21945-970, Brazil

²Department of Physics, University at Buffalo, SUNY, Buffalo, NY 14260-1500

³Instituto de Física, Universidade Federal Fluminense, Niterói, 24210-340, Brazil

⁴Condensed Matter Theory Center, Department of Physics,
University of Maryland, College Park, MD 20742-4111

Abstract

Silicon-based quantum computer architectures have attracted attention because of their promise for scalability and their potential for synergetically utilizing the available resources associated with the existing Si technology infrastructure. Electronic and nuclear spins of shallow donors (e.g. phosphorus) in Si are ideal candidates for qubits in such proposals due to the relatively long spin coherence times. For these spin qubits, donor electron charge manipulation by external gates is a key ingredient for control and read-out of single-qubit operations, while shallow donor exchange gates are frequently invoked to perform two-qubit operations. More recently, charge qubits based on tunnel coupling in P_2^+ substitutional molecular ions in Si have also been proposed. We discuss the feasibility of the building blocks involved in shallow donor quantum computation in silicon, taking into account the peculiarities of silicon electronic structure, in particular the six degenerate states at the conduction band edge. We show that quantum interference among these states does not significantly affect operations involving a single donor, but leads to fast oscillations in electron exchange coupling and on tunnel-coupling strength when the donor pair relative position is changed on a lattice-parameter scale. These studies illustrate the considerable potential as well as the tremendous challenges posed by donor spin and charge as candidates for qubits in silicon.

Key words: semiconductors, quantum computation, nanoelectronic devices, spintronics, nanofabrication, donors in silicon.

I. INTRODUCTION

Most of the computer-based encryption algorithms presently in use to protect systems accessible to the public, in particular over the Internet, rely on the fact that factoring a large number into its prime factors is so computationally intensive that it is practically impossible. These systems would be vulnerable if faster factoring schemes became viable. The development by Shor, about a decade ago, of a quantum algorithm that can factorize large numbers exponentially faster than the available classical algorithms [1] thus could make the public key encryption scheme potentially vulnerable, and has naturally generated widespread interest in the study of quantum computing and quantum information processing [2, 3]. The exponential speedup of Shor's algorithm is due to the intrinsic quantum parallelism in the superposition principle and the unitary evolution of quantum mechanics. It implies that a computer made up of entirely quantum mechanical parts, whose evolution is governed by quantum mechanics, would be able to carry out in reasonably short time prime factorization of large numbers that is prohibitively time-consuming in classical computation, thus revolutionizing cryptography and information theory. Since the invention of Shor's factoring algorithm, it has also been shown that error correction can be done to a quantum system [4], so that a practical quantum computer (QC) does not have to be forever perfect to be useful, as long as quantum error corrections can be carried out. These two key mathematical developments have led to the creation of the new interdisciplinary field of quantum computation and quantum information.

The elementary unit of a QC is the quantum bit, or qubit, which is a two-level quantum system ($|0\rangle$ and $|1\rangle$). Contrary to a classical bit which is in one of the binary states, either 0 or 1, the state of a qubit could be any quantum mechanical superposition state of this two-level system: $\alpha|0\rangle + \beta|1\rangle$, where α and β are complex numbers constrained to the normalization $|\alpha|^2 + |\beta|^2 = 1$. The computation process in a QC consists of a sequence of operations, or logical gates, in terms of locally tailored Hamiltonians, changing the states of the qubits through quantum mechanical evolution. Quantum computation generally involves logical gates that may affect the state of a single qubit, i.e. changing $f_{in, in}$ into $f_{out, out}$, as well as multiple-qubit gates. The formalism for quantum information processing is substantially simplified by the following result proven by Barenco et al [5]: A universal set of gates, consisting of all one-qubit quantum gates and a single two-qubit gate,

e.g. the controlled-NOT (C-NOT) gate, may be combined to perform any logic operation on arbitrarily many qubits.

The physical realization of qubits begins with demonstration of one-qubit gates and the C-NOT quantum gate for one and two qubits. After successfully performing these basic logic operations at the one and two qubits stage, the next step is to scale up, eventually achieving a large scale QC of 10^6 qubits. So far, 15 is the largest number for which Shor's factorization was implemented in a physical system [6]. This factorization required coherent control over seven qubits.

Many physical systems have been proposed as candidates for qubits in a QC, ranging from those in atomic physics, optics, to those in various branches of condensed matter physics [3]. Among the more prominent solid state examples are electron or nuclear spins in semiconductors [7, 8], including electron spin in semiconductor quantum dots [9, 10] and donor electron or nuclear spins in semiconductors [11, 12, 13].

Silicon donor-based QC schemes are particularly attractive because doped silicon makes a natural connection between present microelectronic devices and perspective quantum mechanical devices. Doping in semiconductors has had significant technological impact for the past fifty years and is the basis of current mostly silicon-based microelectronics technology. As transistors and integrated circuits decrease in size, the physical properties of the devices are becoming sensitive to the actual configuration of impurities [14]. In this context, the first proposal of donor-based silicon quantum computer (QC) by Kane [11], in which the nuclear spins of the monovalent ^{31}P impurities in Si are the qubits, has naturally created considerable interest in revisiting all aspects of the donor impurity problem in silicon, particularly in the Si^{31}P system.

In principle, both spin and electronic orbital degrees of freedom can be used as qubits in semiconductor nanostructures. A great advantage of orbital (or equivalently, charge) qubits is that qubit-specific measurements are relatively simple because measuring single charge states involves well-developed experimental techniques using single-electron transistors (SET) or equivalent devices [15]. A major disadvantage of solid state charge qubits is that these orbital states are highly susceptible to interactions with the environment that contains all the stray or unintended charges inevitably present in the device, so that the decoherence time is generally far too short (typically picoseconds to nanoseconds) for quantum error correction to be useful. A related problem is that inter-qubit coupling, which is

necessary for the implementation of two-qubit gate operations essential for quantum computation, is often the long-range dipolar coupling for charge qubits. This makes it difficult to scale up the architecture, since decoherence grows with the scaling-up as more and more qubits couple to each other via the long-range dipolar coupling. However, the strong interactions make the orbital states an excellent choice for studying qubit dynamics and qubit coupling in the solid state nanostructure environment.

Spin qubits in semiconductor nanostructures have complementary advantages (and disadvantages) compared with charge qubits based on quantized orbital states. A real disadvantage of spin qubits is that a single electron spin (not to mention a single nuclear spin) is difficult to measure rapidly, although there is no fundamental principle against the measurement of a Bohr magneton. The great advantage of spin qubits is the very long spin coherence times, which even for electron spins can be milliseconds in silicon at low temperatures. In addition to the coherence advantage, spin qubits also have a considerable advantage that the exchange gate [9], which provides the inter-qubit coupling, is exponentially short-ranged and nearest-neighbor in nature, thus allowing precise control and manipulation of two-qubit gates. There is no fundamental problem arising from the scaling-up of the QC architecture since exchange interaction couples only two nearest-neighbor spin qubits independent of the number of qubits.

We provide here a brief perspective on spin and charge qubits in silicon with electron spins or charge states in shallow P donor levels in Si being used as qubits. In Sec. II we present some background on the classic problem of the shallow donor in silicon, describing it through two complementary approaches: The effective mass theory and the tight-binding formalism. In Sec. III we analyze the response of the donor electron to an applied uniform electric field, and conclude that electric field control over the donor electron does not present additional complications due to the Si host electronic structure characteristics. Sec. IV is devoted to the exchange coupling for a donor pair in Si, which is highly sensitive to interdonor positioning. We review the basic formalism leading to this behavior, and also describe attempts to overcome it, namely by considering donors in strained Si, and by refining the theoretical formalism for the problem. The feasibility of charge qubits based on P_2^+ molecular ions in Si is investigated in Sec. V, where we focus on the tunnel coupling and charge coherence in terms of electron-phonon coupling.

II. SINGLE DONOR IN SILICON

Silicon is a group-IV element, so that when a Si atom at a lattice site R_0 in the bulk is replaced by a group-V element like P, the simplest description for the electronic behavior of the additional electron is a hydrogenic model, in which this electron is subject to the Si crystal potential perturbed by a screened Coulomb potential produced by the impurity ion:

$$V(r) = -\frac{e^2}{\epsilon r} : \quad (1)$$

The static dielectric constant of Si, $\epsilon = 12.1$, indicates that the donor confining potential is weaker than the bare hydrogen atom potential, leading to larger effective Bohr radii and smaller binding energies, so that donors are easily ionized (also known as shallow donors).

In this section we briefly review basic properties concerning the donor ground state wavefunction within two complementary formalisms: The effective mass theory (EMT), which is a reciprocal space formalism, and the tight-binding (TB) formalism, which is a real space scheme. EMT exploits the duality between real and reciprocal space, where delocalization in real space leads to localization in k -space. Since shallow donor wavefunctions are expected to extend over several lattice constants in real space (the lattice parameter of Si crystal is $a_{\text{Si}} = 0.357 \text{ nm}$), it is written in terms of the bulk eigenstates for one or a few k -vectors at the lower edge of the conduction band. The TB description is a microscopic atomistic formalism, in which the basis set for the donor wavefunction expansion consists of atomic orbitals localized at the individual atoms.

A. Effective mass theory

The bound donor electron Hamiltonian for an impurity at site R_0 is written as

$$H_0 = H_{\text{SV}} + H_{\text{VO}} : \quad (2)$$

The first term, H_{SV} , is the single-valley Kohn-Luttinger Hamiltonian [16], which includes the single particle kinetic energy, the Si periodic potential, and the screened impurity Coulomb potential in Eq. (1). The second term of Eq. (2), H_{VO} , includes the inter-valley coupling effects due to the presence of the impurity potential.

Following the EMT assumptions, the donor electron eigenfunctions are written on the basis of the six unperturbed Si band edge Bloch states $\psi_{\mathbf{k}} = u(\mathbf{r})e^{i\mathbf{k} \cdot \mathbf{r}}$ [the conduction

band of bulk Si has six degenerate minima ($\ell = 1; \dots; 6$), located along the X axes of the Brillouin zone at $\mathbf{k} = 0.85(2\pi/a_i)$ from the Γ point]:

$$\psi_{R_0}(\mathbf{r}) = \frac{1}{\sqrt{6}} \sum_{\ell=1}^6 F_{\ell}(\mathbf{r} - \mathbf{R}_0) u_{\ell}(\mathbf{r}) e^{ik_{\ell}(\mathbf{r} - \mathbf{R}_0)} : \quad (3)$$

In Eq. (3), $F_{\ell}(\mathbf{r} - \mathbf{R}_0)$ are envelope functions centered at \mathbf{R}_0 , for which we adopt the anisotropic Kohn-Luttinger form, e.g., for $\ell = z$, $F_z(\mathbf{r}) = \exp[-(x^2 + y^2)/a^2 + z^2/b^2]^{1/2} \sqrt{\frac{2}{a^2 b}}$. The effective Bohr radii a and b are variational parameters chosen to minimize $E_{SV} = \langle \psi_{R_0} | H_{SV} | \psi_{R_0} \rangle$, leading to $a = 25 \text{ \AA}$, $b = 14 \text{ \AA}$, in agreement with the expected increased values with respect to bare atoms.

The H_{SV} ground state is six-fold degenerate. This degeneracy is lifted by the valley-orbit interactions included here in H_{VO} , leading to the nondegenerate (A_1 -symmetry) ground state in (3). Fig. 1 gives the charge density $|\psi_{R_0}(\mathbf{r})|^2$ for this state, where the periodic part of the conduction band edge Bloch functions were obtained from ab-initio calculations, as described in Ref. 17. The impurity site \mathbf{R}_0 , corresponding to the higher charge density, is at the center of the frame. It is interesting that, except for this central site, regions of high charge concentration and atomic sites do not necessarily coincide, because the charge distribution periodicity imposed by the plane-wave part of the Bloch functions is $2\pi/k$, incommensurate with the lattice period.

B. Tight-binding description for P donor in silicon

The TB Hamiltonian for the impurity problem is written as:

$$H = \sum_{ij} \sum_{\sigma} h_{ij} c_{i\sigma}^{\dagger} c_{j\sigma} + \sum_i U(\mathbf{R}_i) c_{i\uparrow}^{\dagger} c_{i\uparrow} \quad (4)$$

where i and j label the atomic sites, $c_{i\sigma}^{\dagger}$ and $c_{i\sigma}$ denote the atomic orbitals and spins, and $c_{i\sigma}^{\dagger}$; $c_{i\sigma}$ are creation and annihilation operators for the atomic states. We do not include spin-orbit corrections, thus all terms are spin-independent. The matrix elements h_{ij} define the on-site energies and first and second neighbors hopping for the bulk material, for which we take the parametrization given in Ref. 18. The donor impurity potential is included in the perturbation term $U(\mathbf{R}_i)$, the same as Eq. (1), but in a discretized form restricted to the lattice sites:

$$U(\mathbf{R}_i) = \frac{e^2}{\epsilon_i} ; \quad (5)$$

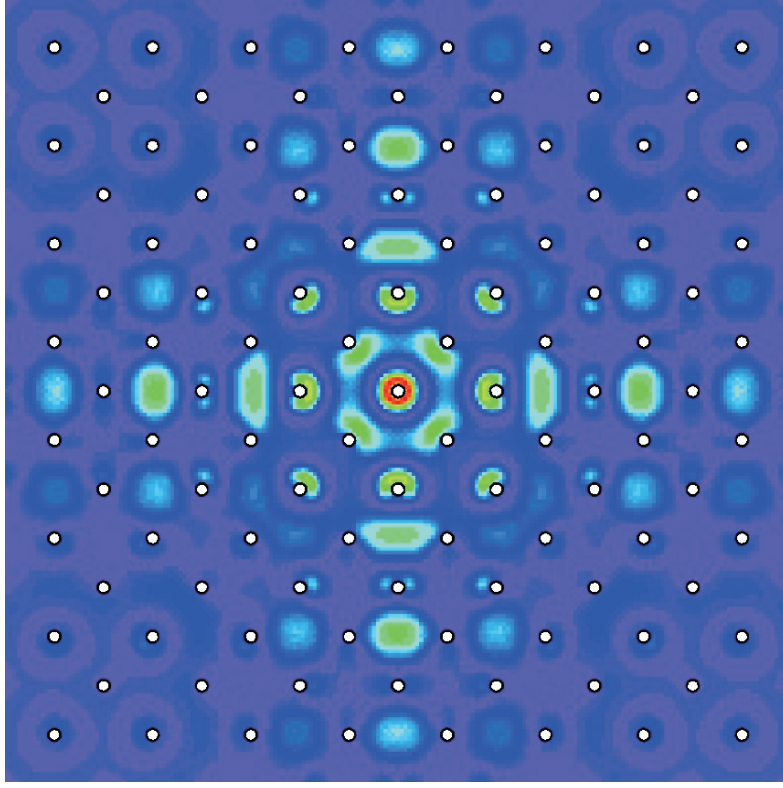


FIG. 1: (Color) Electron probability density on the (001) plane of bulk Si for the ground state of a donor in Si within the Kohn-Luttinger effective mass theory. The white dots give the in-plane atomic sites.

where r_i is the distance of site i to the impurity site. At the impurity site ($r_i = 0$), the perturbation potential is assigned the value U_0 , a parameter describing central cell effects characteristic of the substitutional species. We take $U_0 = 1.48$ eV, which leads to the experimentally observed binding energy of P in Si, 45.6 meV [19]. Detailed comparison of the TB donor ground state wavefunction with Kohn-Luttinger EMT, performed in Ref. 19, shows that the EMT oscillatory behavior coming from the interference among the plane-wave part of the six Γ_6 is well captured by the TB envelope function. The good agreement between TB and K & L is limited to distances from the impurity site larger than a few lattice parameters (~ 1 nm). Closer to the impurity, particularly at the impurity site, the TB results become considerably larger than the K & L prediction, in agreement with experiment.

The TB problem is numerically solved by restricting the real-space description to a supercell in which periodic boundary conditions are applied. For the single donor problem, the supercell is taken to be large enough so that convergence in the results is achieved [19, 20].

III. ELECTRIC FIELD CONTROL OF SHALLOW DONOR IN SILICON

Logic operations in quantum computer architectures based on P donors in Si involve the response of the bound electron wavefunctions to voltages applied to a combination of metal gates separated by a barrier material (e.g. SiO_2) from the Si host. The A-gate (according to the nomenclature originally proposed by Kane [11]), placed above each donor site, pulls the electron wavefunction away from the donor, aiming at partial reduction [11] or total cancellation [21] of the electron-nuclear hyperfine coupling in architectures where the qubits are the ^{31}P nuclear spins. In a related proposal based on the donor electron spins as qubits [13], the gates drive the electron wavefunction into regions of different g-factors, allowing the exchange coupling between neighboring electrons to be tuned.

We present here a simplified model of the A-gate operation by considering the Si:P system under a uniform electric field and near a barrier. Following Ref. 19, we describe the electronic problem within the TB approach, where the basic Hamiltonian is given in Eq. (4), with the perturbation term including the Coulomb potential as in Eq. (5), plus the contribution of a constant electric field of amplitude E applied along the [001] direction:

$$U(\mathbf{R}_i) = \frac{e^2}{\epsilon} \sum_j \mathbf{p}_j \cdot \mathbf{E} \mathbf{z}_j \quad (6)$$

The overall perturbation potential along the z-axis is represented in Fig. 2. We take the origin of the potential at the impurity site, \mathbf{R}_0 , at the center of the supercell. Periodic boundary conditions lead to a discontinuity in the potential at the supercell boundary $z_i = Z_B$, where Z_B is half of the supercell length along [001] or, equivalently, the distance from the impurity to the Si/barrier interface. The potential discontinuity, $V_B = 2\mathbf{p} \cdot \mathbf{E} Z_B$, actually has a physical meaning in the present study: It models the potential due to the barrier material layer above the Si host (see Fig. 2).

A description of the A-gate operations may be inferred from the behavior of the TB envelope function squared (this function is defined at each lattice site as the sum of the squared TB wavefunction expansion coefficients at this site) at the impurity site under applied field E , normalized to the zero-field value:

$$A/A_0 = \sum_{\mathbf{T}_B} \frac{E}{E_0} (\mathbf{R}_0) \sum_j \frac{E}{E_0} (\mathbf{R}_0) \sum_j \quad (7)$$

The notation here indicates that this ratio should follow a behavior similar to that for the hyperfine coupling constants between the donor nucleus and electron with (A) and without

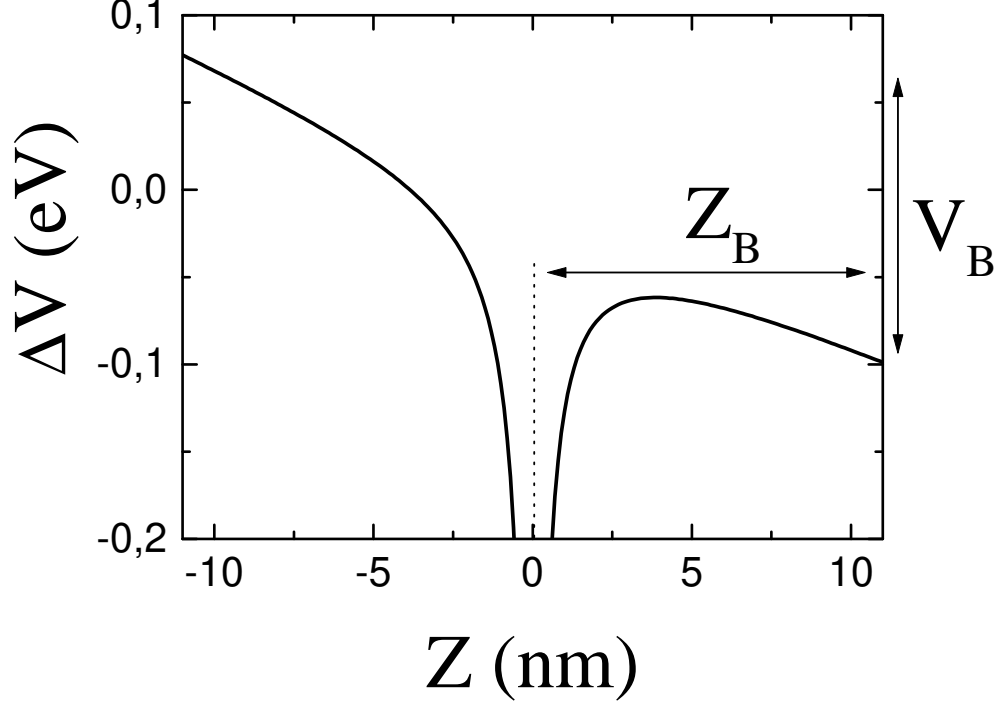


FIG. 2: Schematic representation of the perturbation potential along the z -axis to be added to the bulk Si Hamiltonian due to the impurity at $R = 0$ and to a uniform electric field in the negative z direction. This particular plot corresponds numerically to a supercell length of $L_z = 40a_{\text{Si}}$ and to an electric field of 80 kV/cm .

(A_0) external field. The ratio in (7) is plotted in Fig. 3 (a) for three values of the impurity depth with respect to the Si/barrier interface. Calculations for $Z_B = 10.86 \text{ nm}$ were performed with cubic supercells ($L = 40 a_{\text{Si}}$), while for $Z_B = 5.43$ and 21.72 nm tetragonal supercells with $L_x = L_y = 40 a_{\text{Si}}$ and $L_z = 20 a_{\text{Si}}$ and $80 a_{\text{Si}}$ respectively were used. At small field values we obtain a quadratic decay of $A = A_0$ with E , in agreement with the perturbation theory results for the hydrogen atom. At large enough fields, $j_{\text{TB}}^E(R_0)^2$ becomes vanishingly small, and the transition between the two regimes is qualitatively different according to Z_B : For the largest values of Z_B we get an abrupt transition at a critical field E_c , while smaller Z_B (e.g. $Z_B = 5.43 \text{ nm}$) lead to a smooth decay, similar to the one depicted in Ref. 11. In this latter case, we define E_c as the field for which the curve $A = A_0$ vs E has an inflection point, where $A = A_0 = 0.5$, thus $E_c(5.43 \text{ nm}) = 130 \text{ kV/cm}$. We find that the decrease of E_c with Z_B follows a simple rule $E_c / 1/Z_B$, as given by the solid line in Fig. 3 (b).

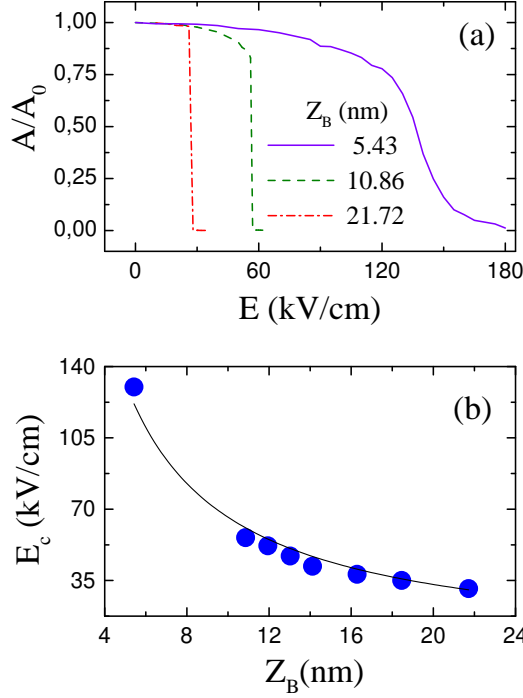


FIG. 3: (a) TB envelope function squared at the impurity site under applied field E , normalized to the zero-field value, for the indicated values of the impurity-Si/barrier interface distance Z_B . (b) Dependence of the critical field E_c on Z_B . The solid line is a best fit of the form $E_c / \sqrt{1+Z_B}$.

The above results may be understood within a simple picture of the electron in a double well potential, the first well being most attractive at the impurity site, $V(R_0 = 0) = -U_0$, and the second well at the barrier interface, $V(z = Z_B) = -V_B/2 = -\frac{1}{2}eE Z_B$ neglecting the Coulomb potential contribution at the interface. An internal barrier separates the two wells and, for a fixed E , this internal barrier height and width increase with Z_B . Deep donor positioning leads to a weaker coupling between the states localized at each well, even close to level degeneracy, resulting the level crossing behavior of the two lowest donor-electron states illustrated in Fig. 4 (a). For a donor positioned closer to the interface, the internal barrier gets weaker, enhancing the coupling between levels localized in each well and leading to wavefunction superposition and to the anticrossing behavior illustrated in Fig. 4 (b). The scaling of E_c with $1/\sqrt{1+Z_B}$ may also be understood assuming that the critical field corresponds to the crossing of the ground state energies of two wells: The Coulomb potential well and an approximately triangular well at the barrier. Since the relative depths of the wells increases

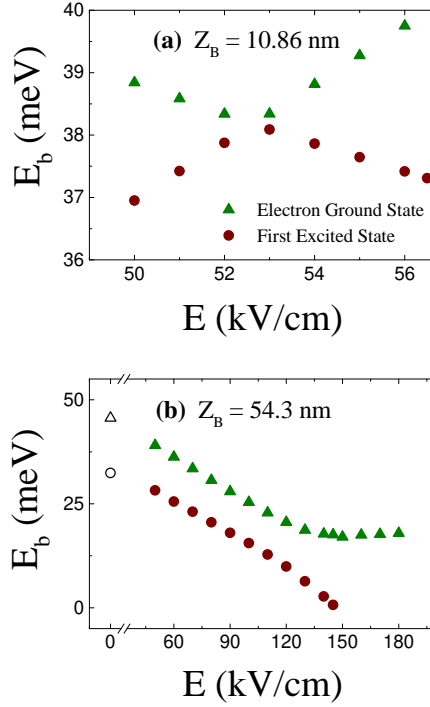


FIG. 4: Calculated binding energies versus electric field intensity of the two lowest donor electron states. (a) For $Z_B = 10.86$ nm the energies reveal a crossing regime. (b) Anticrossing of the two lowest electron states for $Z_B = 54.3$ nm. The open symbols correspond to the zero field calculated values: 45.6 meV and 32.4 meV, in good agreement with experiment.

with $E Z_B$, and assuming that the ground states energies are fixed with respect to each well's depth, the $E_c / 1/Z_B$ behavior naturally results.

The minimum gap at the anticrossing in Fig. 4 (b) is ~ 9.8 meV, which allows for adiabatic control of the electron by the A-gate within switching times of the order of picoseconds, as discussed in Ref. [19]. This is a perfectly acceptable time for the operation of A-gates in spin-based SiQC, given the relatively long electron spin coherence times (of the order of a few ns) in Si.

We remark that the Bloch phases interference behavior in the donor wavefunctions are well captured in the TB wavefunctions, and that the results above demonstrate that electric field control over single donor wavefunctions, such as proposed in A-gate operations, [11, 13, 21] do not present additional complications due to the Si band structure. The only critical parameter is the donor positioning below the Si/barrier interface, which should be chosen

and controlled according to physical criteria such as those discussed here.

IV. DONOR ELECTRON EXCHANGE IN SILICON

An important issue in the study of donor-based SiQC architecture is coherent manipulations of spin states as required for the quantum gate operations. In particular, two-qubit operations, which are required for a universal QC, involve precise control over electron-electron exchange [9, 11, 13, 22]. Such control can presumably be achieved by fabrication of donor arrays with well-controlled positioning and surface gate potential [23, 24, 25, 26]. However, electron exchange in bulk silicon has spatial oscillations [27, 28] on the atomic scale due to valley interference arising from the particular six-fold degeneracy of the bulk Si conduction band. These exchange oscillations place heavy burdens on device fabrication and coherent control [28], because of the very high accuracy and tolerance requirements for placing each donor inside the Si unit cell, and/or for controlling the external gate voltages.

The potentially severe consequences of the exchange-oscillation problem for exchange-based SiQC architecture motivated us and other researchers to perform theoretical studies with increasingly sophisticated formalisms, incorporating perturbation effects due to applied strain [29] or gate fields [30]. These studies, all performed within the standard Heitler-London (HL) formalism [31], essentially reconfirm the originally reported difficulties [28] regarding the sensitivity of the electron exchange coupling to precise atomic-level donor positioning, indicating that they may not be completely overcome by applying strain or electric fields. The sensitivity of the calculated exchange coupling to donor relative position originates from interference between the plane-wave parts of the six degenerate Bloch states associated with the Si conduction-band minima. More recently [17] we have assessed the robustness of the HL approximation for the two-electron donor-pair states by relaxing the phase pinning at donor sites.

In this section, we first review the main results regarding exchange coupling for a donor pair in relaxed bulk Si, and its high sensitivity to interdonor positioning. We then discuss ways to overcome this behavior, namely considering donors in strained Si and the more general rotating-phase HL formalism. We show that strain may partially alleviate the exchange oscillatory behavior, but it cannot entirely overcome the problem. From the rotating-phase HL approach results, our main conclusion is that, for all practical purposes, the previously

adopted HL wavefunctions are robust, and the exchange sensitivity to donor positioning obtained in Refs. 28, 29, 30 persists in the more sophisticated theory of Ref. 17.

A . Donor Electron Exchange in Relaxed Bulk Silicon

The HL approximation is a reliable scheme to calculate electron exchange for a well-separated pair of donors (interdonor distance much larger than the donor Bohr radii) [31]. Within HL, the lowest energy singlet and triplet wavefunctions for two electrons bound to a donor pair at sites R_A and R_B , are written as properly symmetrized and normalized combinations of ψ_{R_A} and ψ_{R_B} [as defined in Eq.(3)]

$$\psi_{\pm}^s(r_1; r_2) = \frac{1}{\sqrt{2(1 \pm S^2)}} [\psi_{R_A}(r_1) \psi_{R_B}(r_2) \pm \psi_{R_B}(r_1) \psi_{R_A}(r_2)]; \quad (8)$$

where S is the overlap integral and the upper (lower) sign corresponds to the singlet (triplet) state. The energy expectation values for these states, $E_{\pm}^s = \langle \psi_{\pm}^s | H | \psi_{\pm}^s \rangle$, give the exchange splitting through their difference, $J = E_{\pm}^s - E_{\mp}^s$. We have previously derived the expression for the donor electron exchange splitting [17, 29], which we reproduce here:

$$J(R) = \frac{1}{36} \sum_{\mathbf{k}} J_{\pm}(R) \cos(\mathbf{k} \cdot \mathbf{R}); \quad (9)$$

where $\mathbf{R} = \mathbf{R}_A - \mathbf{R}_B$ is the interdonor position vector and $J_{\pm}(R)$ are kernels determined by the envelopes and are slowly varying functions of R [28, 29]. Note that Eq. (9) does not involve any oscillatory contribution from $u_{\pm}(r)$, the periodic part of the Bloch functions [17, 30]. The physical reason for that is clear from (3): While the plane-wave phases of the Bloch functions are pinned to the donor sites, leading to the cosine factors in (9), the periodic functions u_{\pm} are pinned to the lattice, regardless of the donor location.

As an example of the consequences of the sensitivity of exchange to interdonor relative positioning, we present in Fig. 5 (a) a case of practical concern involving unintentional donor displacements into nearest-neighbor sites, when the two donors belong to different fcc sublattices. The open squares in Fig. 5 (a) give $J(R)$ for substitutional donors along the [100] axis, while the open triangles illustrate the different-sublattice positioning situation, namely $\mathbf{R} = \mathbf{R}_0 + \tilde{\mathbf{r}}_{NN}$ with \mathbf{R}_0 along the [100] axis and $\tilde{\mathbf{r}}_{NN}$ ranging over the four nearest-neighbors of each \mathbf{R}_0 ($d_{NN} = \sqrt{3} a_{Si} / 2 = 2.34 \text{ \AA}$). The lower panel of the figure presents the

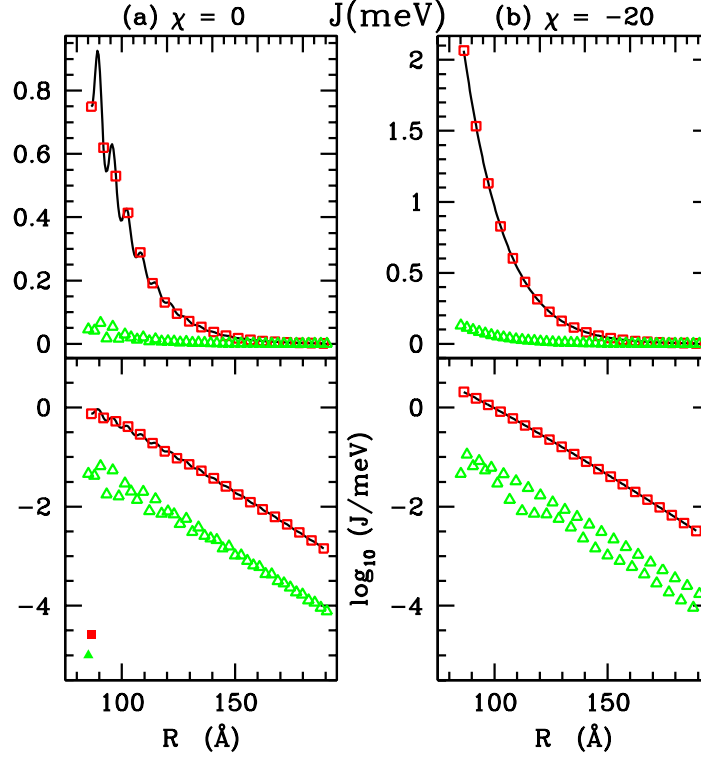


FIG. 5: Calculated exchange coupling for a donor pair versus interdonor distance in (a) unstrained and (b) uniaxially strained (along z) Si. The open squares correspond to substitutional donors placed exactly along the $[100]$ axis, the lines give the calculated values for continuously varied interdonor distance along this axis, assuming the envelopes do not change. The open triangles give the exchange for a substitutional pair almost along $[100]$, but with one of the donors displaced by $d_{NN} = 2.3 \text{ \AA}$ into a nearest-neighbor site. The lower frames give the same data in a logarithmic scale. When the coating-phase HL approach is adopted, the results change negligibly; the filled symbols on the lower left frame give examples of calculated corrections (see text).

same data on a logarithmic scale, showing that nearest-neighbor displacements lead to an exchange coupling reduction by one order of magnitude when compared to $J(R_0)$.

B. Strained Si

The extreme sensitivity of $J(R)$ to interdonor positioning can be eliminated for on-lattice substitutional impurities in uniaxially strained Si (e.g. along the z axis) commensurately grown over Si-Ge alloys if inter-donor separation R remains parallel to the interface x - y plane

[29]. The strain is accommodated in the Si layer by increasing the bond-length components parallel to the interface and decreasing those along z , breaking the cubic symmetry of the lattice and lowering the six-fold degeneracy of the conduction band minimum to two-fold. In this case, the valley populations in the donor electron ground state wave function in Eq. (3) are not all equal to $1/\sqrt{6}$, but are determined from a scalar valley strain parameter ϵ , which quantifies the amount of strain. Fig. 5(b) gives $J(R)$ in uniaxially strained (along z direction) Si for $\epsilon = 20$ (corresponding to Si grown over a Si-Ge alloy with 20% Ge-content) for the same relative positioning of the donor pairs as in Fig. 5(a). Notice that the exchange coupling is enhanced by about a factor of 2 with respect to the relaxed Si host, but the order-of-magnitude reduction in J caused by displacements of amplitude d_{NN} into nearest-neighbor sites still persists as \tilde{r}_{NN} is not parallel to the x - y plane.

C. Floating-phase Heitler-London approach

In Refs. 28 and 29, as in the standard HL formalism presented in subsection IV-A, it is implicitly assumed that the phases $e^{ik \cdot R_0}$ in Eq. (3) remain pinned to the respective donor sites $R_0 = R_A$ and R_B , as we adopt single donor wavefunctions to build the two-electron wavefunction. Although phase pinning to the donor substitutional site is required for the ground state of an isolated donor (A_1 symmetry) in order to minimize single electron energy, this is not the case for the lower-symmetry problem of the donor pair. In order to minimize the energy of the two-donor system, here we allow the phases to shift by an amount R along the direction of the interdonor vector $R = R_B - R_A$, so that the single-particle wavefunctions in Eq. (8) become

$$\psi_{R_A}(r) = \frac{1}{\sqrt{6}} \sum_{\alpha=1}^6 F_{\alpha}(r - R_A) u_{\alpha}(r) e^{ik \cdot (r - R_A + R)} \quad (10)$$

and

$$\psi_{R_B}(r) = \frac{1}{\sqrt{6}} \sum_{\alpha=1}^6 F_{\alpha}(r - R_B) u_{\alpha}(r) e^{ik \cdot (r - R_B - R)} : \quad (11)$$

We take R as a variational parameter to minimize E_s and E_t . Since the phases in Eq.(3) are responsible for the sensitivity of the exchange coupling to donor positioning in Si, this more general variational treatment might lead to changes in the previously reported [28, 29, 30] behavior of the two-donor exchange splitting $J = E_t - E_s$.

Minimization of the total energy for the particular geometry where the donor pair is 87 Å apart along the [100] direction leads the singlet energy decrease of 270 meV, and the triplet energy decrease of 6 meV. This results in an increase in J by 264 meV, given by the solid square in the lower left hand side frame of Fig. 5. The rotating phases variational scheme leads to a reduction in both singlet and triplet states energy, therefore the net variation in J is positive (negative) if the triplet energy reduction is smaller (larger) than the singlet. The solid triangle in Fig. 5 corresponds to a case of negative variation, obtained when one of the donors in the above geometry is displaced into a nearest-neighbor site. Note that the corrections are more than three orders of magnitude smaller than the calculated J within standard HL. In other words, for all practical purposes the fixed-phase standard HL approximation is entirely adequate for the range of interdonor distances of interest for QC applications.

From the perspective of current QC fabrication efforts, 1 nm accuracy in single P atom positioning has been recently demonstrated [24], representing a major step towards the goal of obtaining a regular donor array embedded in single crystal Si. Exchange coupling distributions consistent with such accuracy are presented in Ref. 33, indicating that even such small deviations (1 nm) in the relative position of donor pairs can still lead to significant changes in the exchange coupling, favoring $J = 0$ values. Severe limitations in controlling J would come from "hops" into different substitutional lattice sites. Therefore, precisely controlling of exchange gates in Si remains an open (and severe) challenge. As suggested in Ref. 32, spatially resolved micro-Raman spectroscopy might provide a valuable diagnostic tool to characterize local values of exchange coupling between individual spin qubits.

V. CHARGE QUBITS IN SILICON

Successful coherent manipulation of electron orbital states in GaAs has been achieved for electrons bound to donor impurities [35] as well as electrons in double quantum dots [36]. There were also suggestions of directly using electron orbital states in Si as the building blocks for quantum information processing [37, 38]. Specifically, a pair of phosphorus donors that sit relatively close to each other (so as to have sizable wave function overlap) form an effective hydrogen molecule in Si host material. Charge qubits may be defined by ionizing one

of the bound electrons, thus leading to a double well potential filled with a single electron: The single electron ground state manifold, whether it is the two states localized in each of the wells or their symmetric and anti-symmetric combinations, can then be used as the two-level system forming a charge qubit [39, 40]. The advantage of such a charge qubit is that it is easy to manipulate and detect, while its disadvantage, as already mentioned above, is the generally fast charge decoherence as compared to spin.

In this section we discuss the feasibility of the P_2^+ charge qubit in Si, focusing on single qubit properties in terms of the tunnel coupling between the two phosphorus donors, and charge decoherence of this system in terms of electron-phonon coupling. We take into consideration the multi-valley structure of the Si conduction band and explore whether valley interference could lead to potential problems or advantages with the operations of P_2^+ charge qubits, such as difficulties in the control of tunnel coupling similar to the control of exchange in two-electron systems discussed in Sec. IV, or favorable decoherence properties through vanishing electron-phonon coupling.

A. The P_2^+ molecule in Silicon

We study the simple situation where a single electron is shared by a donor pair, constituting a P_2^+ molecule in Si. The charge qubit here consists of the two lowest energy orbital states of an ionized P_2 molecule in Si with only one valence electron in the outermost shell shared by the two P atoms. The key issue to be examined is the tunnel coupling and the resulting coherent superposition of one-electron states, rather than the entanglement among electrons, as occurs for an exchange-coupled pair of electrons.

The donors are at substitutional sites R_A and R_B in an otherwise perfect Si structure. In the absence of an external bias, we write the eigenstates for the two lowest-energy states as a superposition of single-donor ground state wavefunctions [as given in Eq. (3)] localized at each donor, $\psi_A(r)$ and $\psi_B(r)$, similar to the standard approximation for the H_2^+ molecular ion [31]. The symmetry of the molecule leads to two eigenstates on this basis, namely the symmetric and antisymmetric superpositions

$$\psi_{\pm}(r) = \frac{1}{\sqrt{2}} \frac{\psi_A(r) \pm \psi_B(r)}{(1 \pm S)} : \quad (12)$$

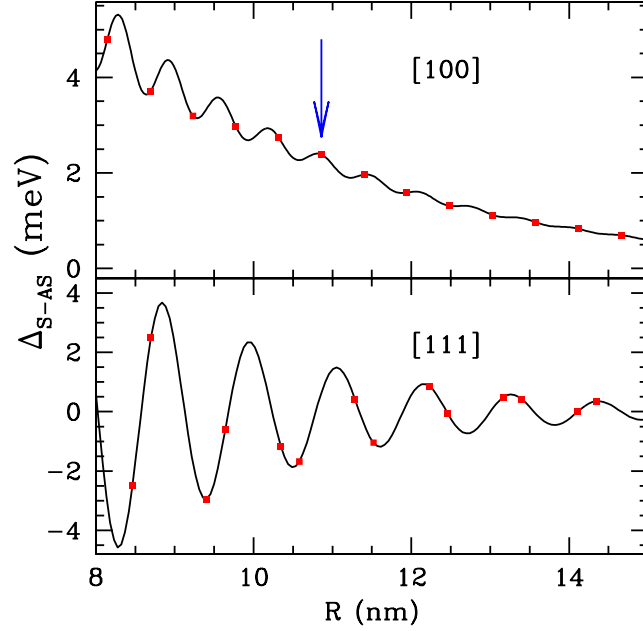


FIG. 6: Symmetric-antisymmetric gap for the P_2^+ molecular ion in Si for the donor pair along the indicated lattice directions. The arrow in the upper frame indicates the target configuration analyzed in Fig. 7.

As described in Ref. 34, the energy gap between these two states may be written as

$$\Delta_{S-AS} = \frac{2}{1 - S^2} \frac{x^6}{=1} (R) \cos(k R) ; \quad (13)$$

where S is the overlap integral between $\psi_A(r)$ and $\psi_B(r)$. For $R = R_A - R_B$ a; b, the amplitudes $\psi(r)$ are monotonically decaying functions of the interdonor distance R , and $S \ll 1$. The dependence of Δ_{S-AS} on R is qualitatively similar to the symmetric-antisymmetric gap in the H_2^+ molecule, namely an exponential decay with power-law prefactors. The main difference here comes from the cosine factors, which are related to the oscillatory behavior of the donor wavefunction in Si arising from the Si conduction band valley degeneracy, and to the presence of two pinning centers.

Fig. 6 shows the calculated gaps as a function of R for a donor pair along two high-symmetry crystal directions. Two points are worth emphasizing here, which are manifestly different from the corresponding hydrogenic molecular ion behavior: (i) Δ_{S-AS} is an

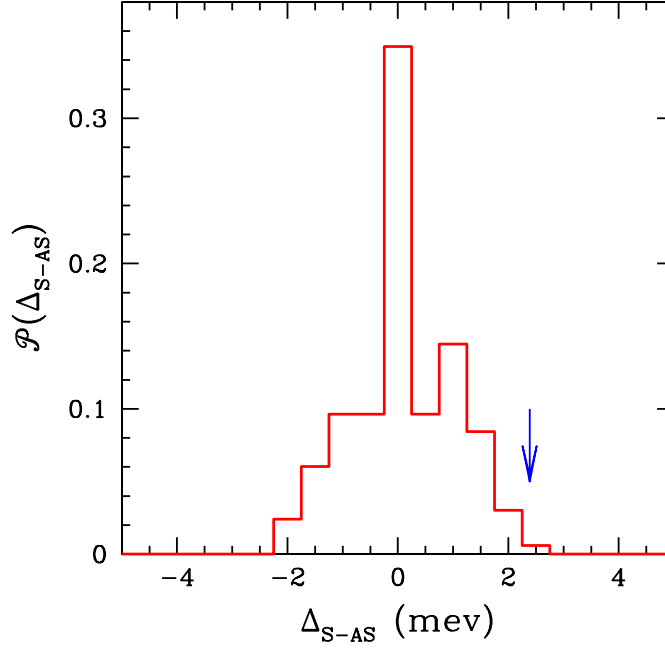


FIG. 7: Probability distribution of the symmetric-antisymmetric gap for the P_2^+ molecular ion in Si. Donor pairs are approximately aligned along $[100]$, but with an uncertainty radius $R_u = 1\text{nm}$ with respect to this target axial alignment (see text). The arrow indicates the gap value for the target configuration, for which the uncertainty radius is $R_u = 0$. Notice that the distribution is peaked at $\Delta_{S-AS} = 0$, and not at the target gap value.

anisotropic and fast oscillatory function of R ; (ii) the sign of Δ_{S-AS} may be positive or negative depending on the precise value of R . The characteristics mentioned in point (i) are similar to the exchange coupling behavior previously discussed for the two-electrons neutral donor pair.[17, 28, 29] Point (ii) implies that the P_2^+ molecular ion ground state in Si may be symmetric (as in the H_2^+ molecular ion case) or antisymmetric depending on the separation between the two P atoms. Note that for the two-electron case, the ground state is always a singlet (i.e. a symmetric two-particle spatial part of the wavefunction with the spin part being antisymmetric), implying that the exchange J is always positive for a two-electron molecule. For a one-electron ionized molecule, however, the ground state spatial wavefunction can be either symmetric or antisymmetric.

Fig. 7 shows the normalized probability distribution for the Δ_{S-AS} gap values when the

first donor is kept fixed at R_A and the second donor is placed at a site 20 lattice parameters away ($\approx 108.6\text{\AA}$), along the $[100]$ axis. This target configuration is indicated by an arrow in Fig. 6. We allow the second donor position R_B to visit all possible substitutional diamond lattice positions within a sphere of radius R_u centered at the attempted position. Our motivation here is to simulate the realistic fabrication of a P_2^+ molecular ion with fixed inter-atomic distance in Si with the state of the art Si technology, in which there will always be a small ($R_u \approx 1 - 3\text{ nm}$) uncertainty in the precise positioning of the substitutional donor atom within the Si unit cell. We would like to estimate the resultant randomness or uncertainty in ϵ_{SAS} arising from this uncertainty in R_B . For $R_u = 0$, i.e., for $R = 20a_{Si}$, $\epsilon_{SAS} \approx 2.4\text{ meV}$, given by the arrows in Fig. 7. We incorporate the effect of small uncertainties by taking $R_u = 1\text{ nm}$, corresponding to the best reported degree of accuracy in single P atom positioning in Si [24]. These small deviations completely change the qubit gap distribution, as given by the histogram in Fig. 7, strongly peaked around zero. Further increasing R_u leads to broader distributions of the gap values, though still peaked at zero [34]. This broadening is due to the fast increase in the number of lattice sites inside the sphere of radius R_u , thus contributing to the distribution, as R_u increases. We conclude that the valley interference between the six Bloch states leads to a strong suppression of the qubit delity since the most probable ϵ_{SAS} tends to be zero.

A very small ϵ_{SAS} is undesirable in defining the two states $|j_i\rangle$ and $|j_l\rangle$ forming the charge qubit. If we take them to be the symmetric and anti-symmetric states given in Eq. (12), the fact that they are essentially degenerate means that, when one attempts to initialize the qubit state at $|j_i\rangle$, a different combination $|j_i\rangle + |j_l\rangle$ might result. Well defined qubits may still be defined under a suitable applied external bias, so that the electron ground state wavefunction is localized around one of the donors, say at lattice site R_A , and the first excited state is localized around R_B .

Single qubit rotations, used to implement universal quantum gates [2], might in principle be achieved by adiabatic tunneling of the electron among the two sites under controlled axially aligned electric fields through bias sweeps [41]. When, at zero bias, the ground state is not well separated by a gap from the first excited state, severe limitations are expected in the adiabatic manipulation of the electron by applied external fields. In other words, the delity of the single qubit system defining the quantum two-level dynamics will be severely compromised by the valley interference effect.

B . Electron-phonon coupling

Two key decoherence channels for charge qubits in solids are background charge fluctuations and electron-phonon coupling [36]. The former is closely related to the sample quality (e.g., existences of stray charges and charged defects in the system) and is extrinsic, while the latter is intrinsic. Here we focus on the electron-phonon coupling. A critical question for the P_2^+ molecular ion in Si is whether the Si band structure and the associated charge density oscillations [17] lead to any significant modification of the electron-phonon coupling matrix elements. The relevant terms for the electron-phonon interaction in Si takes the form :

$$H_{ep} = D \sum_q \frac{\hbar}{2 m V} \sum_{l=1,2} \hat{J}_l(q) (a_q + a_q^\dagger); \quad (14)$$

where D is the deformation constant, m is the mass density of the host material, V is the volume of the sample, a_q and a_q^\dagger are phonon annihilation and creation operators, and $\hat{J}_l(q)$ is the Fourier transform of the electron density operator. For the two-donor situation, where we are only interested in the two lowest energy single-electron eigenstates, the electron-phonon coupling Hamiltonian is conveniently written in this quasi-two-level basis in terms of the Pauli spin matrices σ_x and σ_z (where spin up and down states refer to the two electronic eigenstates, labeled $|f\rangle, |i\rangle$):

$$\begin{aligned} H_{ep} &= D \sum_q \frac{\hbar}{2 m V} \sum_{l=1,2} \hat{J}_l (A_r \sigma_x + A_l \sigma_z) (a_q + a_q^\dagger); \\ A_r &= \hbar \sum_j e^{iq \cdot r_j} \langle f | i \rangle; \\ A_l &= \frac{1}{2} \hbar \sum_j e^{iq \cdot r_j} \langle f | i \rangle - \hbar \sum_j e^{iq \cdot r_j} \langle f | j \rangle \langle j | i \rangle; \end{aligned} \quad (15)$$

Here the term proportional to σ_x can lead to transition between the two electronic eigenstates and is related to relaxation; while the term proportional to σ_z only causes energy renormalization of the two electronic levels, but no state mixing, so that it only leads to pure dephasing for the electronic charge states.

Calculations of the matrix elements involved in Eq. (15), reported in Ref. 34, lead to the conclusion that the electron-phonon coupling for a P_2^+ molecular ion in Si formally behaves very similarly to that for a single electron trapped in a GaAs double quantum dot. For example, the relaxation matrix element is proportional to

$$\begin{aligned} A_r &= \langle ab | \sum_{\mathbf{R}} a b e^{iq \cdot \mathbf{R}} \rangle \int d\mathbf{r} e^{iq \cdot \mathbf{r}} |\Psi(\mathbf{r})|^2 \\ &+ \langle \langle b |^2 - |a|^2 \rangle \rangle \int d\mathbf{r} e^{iq \cdot \mathbf{r}} \Psi^*(\mathbf{r}) \Psi(\mathbf{r} - \mathbf{R}); \end{aligned} \quad (16)$$

where the more complicated multi-valley bandstructure of Si and the strong inter-valley coupling introduced by the phosphorus donor atoms only strongly affect the σ -site (thus small) contribution to the electron-phonon coupling, so that they do not cause significant changes in the overall electron-phonon coupling matrix elements. Therefore, available estimates [41, 42] of decoherence induced by electron-phonon coupling based on a single-valley hydrogenic approximation in the P_2^+ system in Si should be valid. In other words, the multi-valley quantum interference effect does not provide any particular advantage (or disadvantage) for single qubit decoherence in the SiP donor charge-based QC architecture.

VI. SUMMARY

In summary, we have briefly reviewed physical aspects related to some of the relevant building blocks for the implementation of donor spin and charge qubits in silicon: Electric field control of a single donor, the exchange gate for two spin qubit operations, control and coherence of P_2^+ charge qubits. Our results indicate that, although some of the operations may be implemented as originally conceived, the spin and charge qubits based on donors in silicon pose immense challenges in terms of precise nanostructure fabrications because of the degenerate nature of the silicon conduction band. Further studies of fabrication and innovative alternative approaches are imperative in order to fully realize the potential of donor-based QC architectures.

Acknowledgments

This work was supported by Conselho Nacional de Desenvolvimento Científico e Tecnológico (CNPq), Instituto do Milênio de Nanociências and Fundação Carlos Chagas Filho de Amparo à Pesquisa do Estado do Rio de Janeiro (FAPERJ) in Brazil, Advanced Research and Development Authority (ARDA) and Laboratory for Physical Sciences – National Security Agency (LPS-NSA) at the University of Maryland, and by The Army Research Office – Advanced Research and Development Authority (ARO-ARDA) at the University at Buffalo.

and the University of Maryland.

- [1] P. W. Shor, "Polynomial-time algorithms for prime factorization and discrete logarithms on a quantum computer," in: S. Goldwasser ed., *Proceedings of the 35th Annual Symposium on the Foundations of Computer Science* (IEEE Computer Society, Los Alamitos, 1994), 124-134.
- [2] M. A. Nielsen and I. L. Chuang, *Quantum computation and quantum information* (Cambridge Univ. Press, Cambridge, U.K., 2000).
- [3] D. P. DiVincenzo, "Quantum Computation," *Science* 270 (1995) 255; A. Ekert and R. Jozsa, "Quantum computation and Shor's factoring algorithm," *Rev. Mod. Phys.* 68 (1996) 733-753; A. Steane, "Quantum computing," *Rep. Prog. Phys.* 61 (1998) 117-173; C. H. Bennett and D. P. DiVincenzo, "Quantum information and computation," *Nature* 404 (2000) 247-255.
- [4] P. W. Shor, "Scheme for reducing decoherence in quantum computer memory," *Phys. Rev. A* 52 (1995), R2493-R2496; A. M. Steane, "Error correcting codes in quantum theory," *Phys. Rev. Lett.* 77 (1996) 793-797.
- [5] A. Barenco, C. H. Bennett, R. Cleve, D. P. DiVincenzo, N. Margolus, P. Shor, T. Sleator, J. A. Smolin, and H. Weinfurter, "Elementary gates for quantum computation," *Phys. Rev. A* 52 (1995) 3457-3467.
- [6] L. M. K. Vandersypen, M. Steen, G. Breyta, C. S. Yannoni, C. S. M. H. Sherwood, and I. L. Chuang, "Experimental realization of Shor's quantum factoring algorithm using nuclear magnetic resonance," *Nature* 414 (2001) 883-887.
- [7] I. Zutic, J. Fabian, and S. Das Sarma, "Spintronics: Fundamentals and applications," *Rev. Mod. Phys.* 76 (2004) 323-410.
- [8] S. Das Sarma, J. Fabian, I. Zutic, "Spin electronics and spin computation," *Solid State Commun.* 119 (2001) 207-215; X. Hu and S. Das Sarma, "Overview of spin-based quantum dot quantum computation," *Phys. Stat. Sol. (b)* 238 (2003) 360-365; X. Hu, "Quantum Dot Quantum Computing," *arXiv:cond-mat/0411012*; S. Das Sarma, R. de Sousa, X. Hu, B. Koiller, "Spin quantum computation in silicon nanostructures," *Solid State Commun.* 113 (2005) 737-746.
- [9] D. Loss and D. P. DiVincenzo, "Quantum computation with quantum dots," *Phys. Rev. A* 57 (1998) 120-126.

- [10] A. Imamoglu, D.D. Awschalom, G. Burkard, D.P. Divincenzo, D. Loss, M. Sherwin, and A. Small, "Quantum information processing using quantum dot spins and cavity QED," *Phys. Rev. Lett.* 83 (1999) 4204-4207.
- [11] B.E. Kane, "A silicon-based nuclear spin quantum computer" *Nature* 393 (1998) 133-137.
- [12] V.P. Rivkin, I.D. Vagner, and G. Kventse, "Quantum computation in quantum Hall systems," *Phys. Lett. A* 239 (1998) 141-146.
- [13] R. Vrijen, E. Yablonovitch, K. Wang, H.W. Jiang, A. Balandin, V. Roychowdhury, T. Mor, and D.P. Divincenzo, "Electron-spin-resonance transistors for quantum computing in silicon-germanium heterostructures," *Phys. Rev. A* 62 (2000) 012306.
- [14] P.M. Voyles, D.A. Muller, J.L. Grazzi, P.H. Citrin, and H.-J.L. Grossmann, "Atomic-scale imaging of individual dopant atoms and clusters in highly n-type bulk Si," *Nature* 416 (2002) 826-829.
- [15] Single Charge Tunneling, ed. by H. Grabert and M.H. Devoret (Plenum, New York, 1992).
- [16] W. Kohn, "Shallow impurity states in silicon and germanium," in *Solid State Physics*, vol. 5, F. Seitz and D. Turnbull Ed. New York: Academic Press, 1957, pp. 257-320.
- [17] B. Koiller, R.B. Capaz, X. Hu and S. Das Sarma, "Shallow donor wavefunctions and donor-pair exchange in silicon: Ab initio theory and coating-phase Heitler-London approach," *Phys. Rev. B* 70 (2004) 115207.
- [18] G. Klimck, R.C. Bowen, T.B. Boykin, C.S. Lazaro, T.A. Cwik, and A. Stoica, "Sight-binding parameters from genetic algorithm fitting," *Superlattices Microstruct* 27 (2000) 77-88.
- [19] A.S. Martins, R.B. Capaz, and B. Koiller, "Electric field control and adiabatic evolution of shallow-donor impurities in silicon," *Phys. Rev. B* 69 (2004) 085320.
- [20] A.S. Martins, J.G. Menchero, R.B. Capaz, and B. Koiller, "Atomistic description of shallow levels in semiconductors," *Phys. Rev. B* 65 (2002) 245205.
- [21] A.J. Skinner, M.E. Davenport, and B.E. Kane, "Hydrogenic spin quantum computing in silicon: A digital approach," *Phys. Rev. Lett.* 90 (2003) 087901.
- [22] X. Hu and S. Das Sarma, "Hilbert-space structure of a solid-state quantum computer: Two-electron states of a double-quantum-dot artificial molecule," *Phys. Rev. A* 61 (2000) 062301.
- [23] J.L. O'Brien, S.R. Schofield, M.Y. Simmons, R.G. Clark, A.S. Dzurak, N.J. Curson, B.E. Kane, N.S. McAulpine, M.E. Hawley, and G.W. Brown, "Towards the fabrication of phosphorus

- qubits for a silicon quantum computer," *Phys. Rev. B* 64 (2001) 161401.
- [24] S.R. Schofield, N.J. Curson, M.Y. Simmons, F.J. Rue, T. Hallam, L. Oberbeck, and R.G. Clark, "Atomically precise placement of single dopants in Si", *Phys. Rev. Lett.* 91 (2003) 136104.
- [25] T.M. Buehler, R.P. McKinnon, N.E. Lumpkin, R. Brenner, D.J. Reilly, L.D. Marks, A.R. Hamilton, A.S. Durak, and R.G. Clark, "A self-aligned fabrication process for silicon quantum computer devices," *Nanotechnology* 13 (2002) 686-690.
- [26] T. Schenkel, A. Persaud, S.J. Park, J. Nilsson, J. Bokor, J.A. Liddle, R. Keller, D.H. Schneider, D.W. Cheng, and D.E. Humphries, "Solid state quantum computer development in silicon with single ion implantation," *Journal of Applied Physics* 94 (2003) 7017-7024.
- [27] K. Andres, R.N. Bhatt, P. Goalwin, T.M. Rice, and R.E. Walstedt, "Low-temperature magnetic-susceptibility of Si-P in the non-metallic region," *Phys. Rev. B* 24 (1981) 244-260.
- [28] B. Koiller, X. Hu and S. Das Sarma, "Exchange in silicon-based quantum computer architecture," *Phys. Rev. Lett.* 88 (2002) 027903.
- [29] B. Koiller, X. Hu and S. Das Sarma, "Strain effects on silicon donor exchange: Quantum computer architecture considerations," *Phys. Rev. B* 66 (2002) 115201.
- [30] C.J. Wellard, L.C.L. Hollenberg, F. Parisoli, L. Kettle, H.-S. Goan, J.A.L. McIntosh, and D.N. Jamieson, "Electron exchange coupling for single-donor solid-state spin qubits," *Phys. Rev. B* 68 (2003) 195209.
- [31] J.C. Slater, *Quantum Theory of Molecules and Solids*, vol. 1, McGraw-Hill, New York, 1963.
- [32] B. Koiller, X. Hu, H.D. Drew, and S. Das Sarma, "Disentangling the Exchange Coupling of Entangled Donors in the Silicon Quantum Computer Architecture", *Phys. Rev. Lett.* 90 (2003) 067401.
- [33] B. Koiller and X. Hu, "Nanofabrication aspects of silicon-based spin quantum gates", *IEEE Transactions in Nanotechnology* 4 (2004) 113-115.
- [34] X. Hu, B. Koiller, and S. Das Sarma, "Charge qubits in semiconductor quantum computer architectures: Tunnel coupling and decoherence", *arXiv:cond-mat/0412340* (2004), to appear in *Phys. Rev. B*.
- [35] B.E. Cole, J.B. Williams, B.T. King, M.S. Sherwin, and C.R. Stanley, "Coherent manipulation of semiconductor quantum bits with terahertz radiation", *Nature* 410 (2000) 60-63.
- [36] T. Hayashi, T. Fujisawa, H.D. Cheong, Y.H. Jeong, and Y. Hirayama, "Coherent Manipu-

- lation of Electronic States in a Double Quantum Dot", *Phys. Rev. Lett.* 91 (2003) 226804.
- [37] L.C.L. Hollenberg, A.S. Dzurak, C.J. Wellard, A.R. Hamilton, D.J. Reilly, G.J. Milburn, and R.G. Clark, "Charge-based quantum computing using single donors in semiconductors", *Phys. Rev. B* 69 (2004) 113301.
- [38] L.C.L. Hollenberg, C.J. Wellard, C.I. Pakes, and A.G. Fowler, "Single-spin readout for buried dopant semiconductor qubits", *Phys. Rev. B* 69 (2004) 233301.
- [39] A.K. Ekert and R. Jozsa, "Quantum computation and Shor's factoring algorithm", *Rev. Mod. Phys.* 68 (1996) 733-753.
- [40] T. Tanamoto, "One- and two-dimensional N -qubit systems in capacitively coupled quantum dots", *Phys. Rev. A* 64 (2001) 062306; "Quantum gates by coupled asymmetric quantum dots and controlled-NOT-gate operation", *ibid.* 61 (2000) 022305.
- [41] S.D. Barrett and G.J. Milburn, "Measuring the decoherence rate in a semiconductor charge qubit", *Phys. Rev. B* 68 (2003) 155307.
- [42] L. Fedichkin and A. Fedorov, "Error rate of a charge qubit coupled to an acoustic phonon reservoir", *Phys. Rev. A* 69 (2004) 032311.